DIAGNOSIS AND MODELLING OF INTERIOR NOISE IN HELICOPTER CABINS

J. CAILLET*, F. MARROT, F. MALBURET*, J-C. CARMONA***

* **L**aboratoire des **S**ciences de l'**I**nformation et des **S**ystèmes, UMR CNRS 6168
CER ENSAM, 2, cours des Arts et Métiers, 13617 Aix-en-Provence, FRANCE
Contact : julien.caillet@aix.ensam.fr
** EUROCOPTER, service Vibration et Bruit Interne
Aéroport international de Marseille-Provence 13725 Marignane Cedex FRANCE

Abstract :

The main goal of this work is to identify the contributions of noise sources in a helicopter cabin in order to improve the acoustical comfort, by use of passive techniques. Since a complete numerical prediction of the cabin interior noise is not available at medium and high frequencies, this includes both diagnosis and modeling purposes. Cabin noise level in helicopters is mainly due to transmission gearbox, rotor, engines and aerodynamic excitation. These "primary" sources cover a broad frequency range extending within the range of dBSIL4, which is the frequency band at stake here. Disturbances generated by these sources propagate through the airframe and reach into the cabin via airborne and structure-borne energy paths, thus producing radiated noise by the panels of the cabin, acting as "apparent" sources. This study focuses on two problems: the first one is to estimate the contribution of each primary source on the interior level, which can be achieved with conditioned spectral analysis. The second problem is to rank the vibrating panels in the cabin according to their effect upon the inside noise level. A complete system combining measurements by means of Nearfield Acoustical Holography (NAH) and simulation with an acoustical ray-tracing method is then derived as the most suitable one for a reverberant and noisy environment such as an aircraft. The coupling of these tools is assessed successfully on simple test cases and for an in-flight measurement on a whole helicopter cabin.

Introduction:

The work presented in this paper settles in the general framework aiming to improve the acoustical comfort in helicopter cabins, including both diagnosis and modelling purposes, by use of passive techniques (insulating, damping, and porous materials). Cabin noise level in helicopters is mainly due to transmission gearbox, rotor, engines and aerodynamic excitation (See Fig. 1). These "primary" sources cover a broad frequency range extending within the range of dBSIL4 (Speech Interference Level, 4-octave average), which is the frequency band at stake here. This metric rates steady noise, according to its relative ability to interfere with conversation between people.

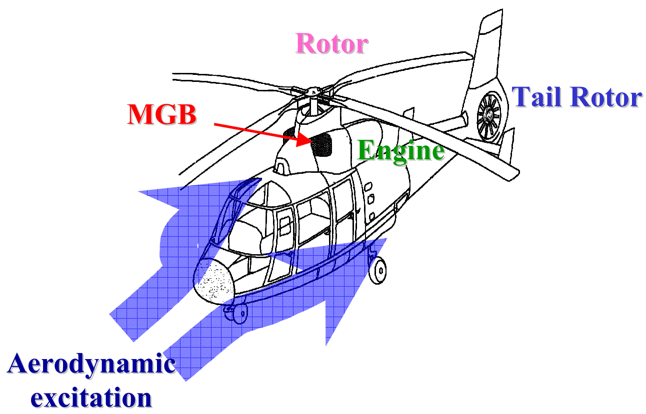

Fig. 1 : Main Noise Sources

Disturbances generated by these sources propagate through the airframe and reach into the cabin via airborne and structure-borne energy paths, thus producing radiated noise by the panels of the cabin, acting as apparent correlated noise sources (Fig.2). From all these involved phenomena, the noise power spectral density in the cabin takes the form of a broadband noise together with a tonal noise at the gearbox mechanical frequencies (See Fig.3).

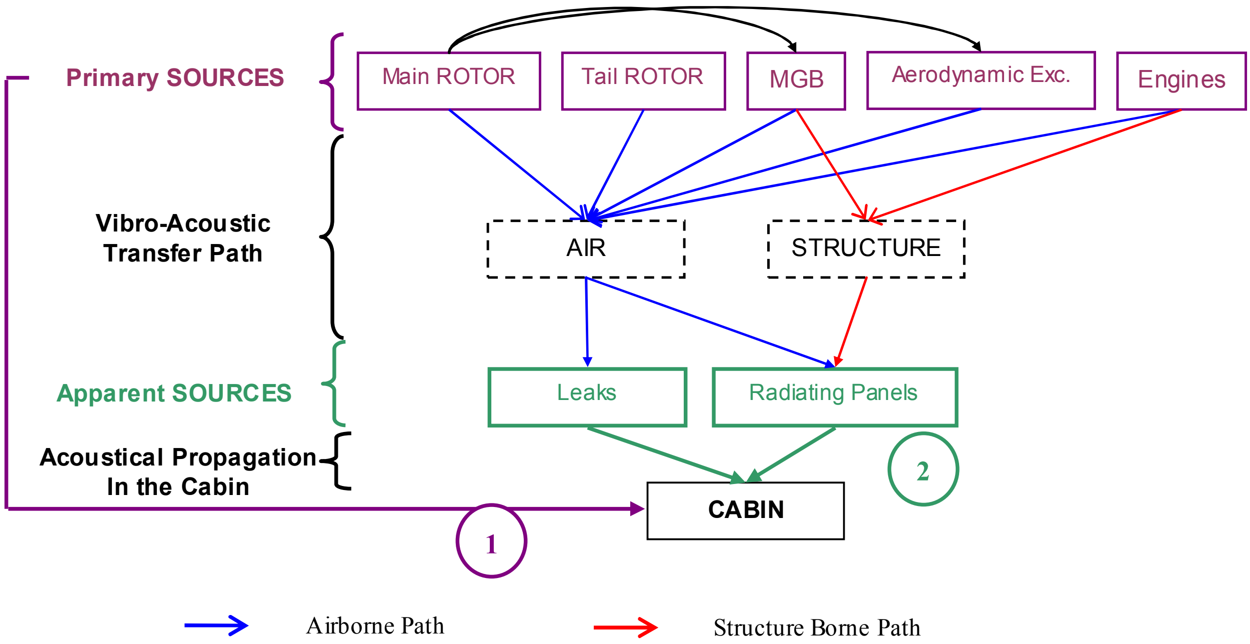

Fig. 2: The Complex Vibro-Acoustic Problem

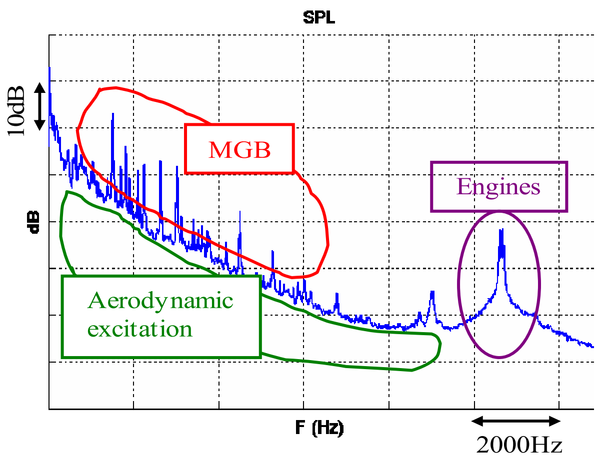

Fig. 3 : Noise PSD inside a helicopter cabin

Two problems are generally associated with the diagnosis problem in a whole vehicle:
According to Fig.2, the first problem (①) is to estimate the contribution of each primary source on the interior level, which can be achieved with conditioned spectra analysis, combined with "pragmatic" in-flight tests. Due to the multi-source environment combined with a multi-path propagation to the cabin, estimating the contribution of each transfer path reveals to be very difficult.
The second problem (②) considered here is to determine how these energy paths propagate and which are the most radiating panels in the helicopter cabin in order to propose some efficient noise reduction technique (trim panels, joints). We also want to locate the acoustical leaks that can be critical for the acoustical comfort in the cabin. This involves both diagnosis and modelling investigations. On one side, the goal of the diagnosis phase is to locate the noise sources and leaks in the cabin. On the other side, simulation objective is to rank these vibrating panels and leaks according to their effect upon the inside noise level.
At the moment, a complete numerical prediction of the cabin interior noise is not available within the proposed frequency range, due to the difficulty of estimating the forces applying to the cabin and the damping of the structure. Moreover, because of the numerous reflexions of the acoustic waves in the cabin, the diagnosis cannot be done with a single microphone measurement.
The objective is thus to define a complete system combining measurements and modelling to get a better knowledge of noise path.
The main radiating zones localisation relies upon in-flight measurements with an acoustical imaging technique to complete the standard spectral analysis with a spatial analysis of the sources. In [1], J-C Pascal pointed out three main methods enabling to spatially represent an acoustical field radiated by a source: Intensimetry, Beamforming and Nearfield Acoustical Holography (NAH).

In [2], the different conceivable diagnostic techniques have been compared on both principles and practical implementation with respect to the helicopter application case. NAH was derived as the most suitable one. The fundamentals of NAH may be found in many scientific publications. Among them, the references [3] and [4] are certainly the most cited in the literature. NAH aims to solve the inverse problem consisting in rebuilding the acoustical field on the interior surface of the cabin from measurements of the pressure on a 2-D handy microphone antenna. One of the advantages of this method is that the normal velocity field can also be obtained.
From a modelling point of view, the objective was to use the in-flight measurement results thus derived, and particularly the acoustical velocity field, to rank the influence of each source upon the interior sound level in the medium and high-frequency range.
Thus, a complete system combining measurements by means of Nearfield Acoustical Holography (NAH) and simulation with an acoustical ray-tracing method have been derived as the most suitable one for a reverberant and noisy environment as an aircraft. The main goal of this paper is to assess the contribution of this approach on the knowledge of helicopter interior noise.

This paper is organized as follows. In a first section of the paper, we present a method to evaluate the contribution of each primary source on the interior noise level, based upon conditioned spectral analysis and on a “pragmatic” analysis. In the second part, we focus on the “apparent” sources problem: we present the chosen methodology aiming at coupling NAH and ray-tracing techniques. In a third part, this coupling is achieved successfully on simple test cases, and both measurement and numerical aspects of the method are validated. NAH capabilities in particularly noisy conditions such as the ones encountered in a helicopter cabin are then evaluated on laboratory condition measurement cases. In a fourth section, holography is assessed on a whole helicopter, with both on ground and in-flight tests. The entire cabin is meshed with stickers and all the panels are measured. Computed acoustic pressure at passenger’s ears locations are compared with microphone measurements. Results are discussed insisting on the contribution of the chosen approach which allows for a better knowledge of the acoustic energy distribution on elementary surfaces such as roofs and openings and a classification of the contribution of the radiating zones on inside sound pressure level.

1. Evaluation of the contribution of the primary sources:

In order to estimate the contribution of each primary source on the interior noise level, several methods can be considered. Due to the multi-source environment combined with a multi-path propagation of the vibro-acoustic energy, we decide to focus on the analysis of signals at receiver positions (in the cabin). A parametric study is performed considering both spatial repartition of the acoustic pressure in the cabin and sound pressure variations due to changes in the flight speed of the helicopter.

This parametric study is coupled with conditioned spectral analysis ([5]) in order to differentiate between aerodynamic noise and main gearbox noise. The conditioning of cabin spectra with MGB spectra is performed with a multiple coherence approach that enables to separate cabin spectra in two parts: one is coherent with MGB signals whereas the second is the aerodynamic contribution which is derived from the difference between total noise and noise from the MGB (in a particular frequency range) according to:

$$S_{CC} = \underbrace{\gamma^2_{C:r_1,r_2,r_3} S_{CC}}_{coherent\ with\ MGB} + \underbrace{(1-\gamma^2_{C:r_1,r_2,r_3}) S_{CC}}_{not\ coherent\ with\ MGB,\ i.e\ aerodynamic\ contribution} \quad (1)$$

$$\gamma^2_{C:r_1,r_2,r_3} = 1-(1-\gamma^2_{Cr_1})(1-\gamma^2_{Cr_2.r_1})(1-\gamma^2_{Cr_3.r_1,r_2}) \quad (2)$$

Where S_{CC} is the total power spectra at a cabin location, $\gamma^2_{C:r1,r2,r3}$ is the multiple coherence of the cabin signal with 3 signals (r_1, r_2, r_3) related to the Main Gearbox. This multiple coherence is derived from equation 2, where $\gamma^2_{x_1x_2.x_3}$ denotes the partial coherence between two signals x_1 and x_2, with the contribution of signal x_3 removed.

From this analysis, we can derive the contribution of MGB and aerodynamic contribution at every position in the cabin and for different speeds. The following fig.4 plots the evolution of aerodynamic power spectral density at the centre of the cabin with speed variations.

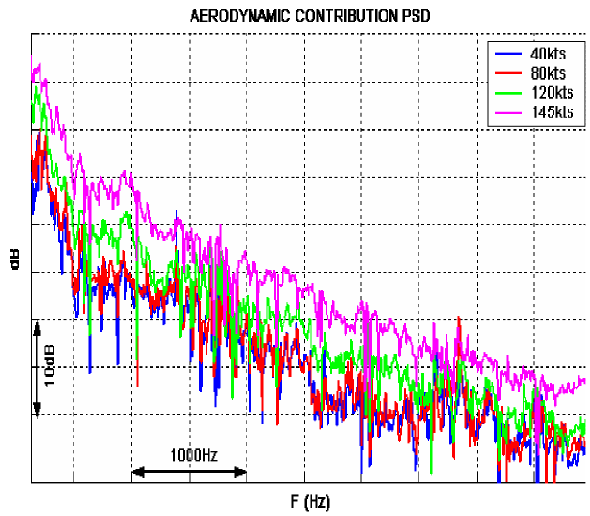

Fig. 4: Aerodynamic Power spectral density evolution

The same analysis can be done with changing microphone position in the cabin. However, tough this analysis gives much information on primary sources contribution, much more attention is paid on the apparent noise sources problem.

2. The apparent noise sources problem: Coupling NAH and Geometrical Acoustics:

2.1 NAH Measurement: NAH aims to solve the inverse problem consisting in rebuilding the acoustical field on the interior surface of the cabin from measurements of the pressure on a handy 2-D microphone antenna, handled close to the studied panel.

In the last decades, NAH has become a powerful tool for the study of noise sources for both exterior and interior problems, such as interior noise in aircrafts. For example, the reference [6] presents an application of NAH to the interior of an airplane Beech 1900D.

The principles of NAH are briefly discussed below. The basic idea is to take advantage of the complexity and richness of the source nearfield information. This is performed by realizing a set of acoustical measurements in a plane which should be parallel and cover the radiating source. The measured signals are supposed to be stationary during the acquisition so that, thanks to the use of a fixed set of references, a complete fictive antenna is artificially built. A diffuse interpolation technique eases the operator from measurement requirements according to regular geometry's (See Ref. [7]). From this complete fictive array measurement, NAH can be divided into three main steps:

-First, the acoustical field measured on the antenna is decomposed in plane waves by application of the two-dimensional (spatial) Fourier transform.

$$P_A(k_x,k_y,z=z_A,\omega)=SFT(p_A(x,y,z,\omega))$$
$$=\frac{1}{(2\pi)^2}\iint_{x,y} p_A(x,y,z=z_A,\omega)e^{j(k_x x+k_y y)}dxdy \qquad (3)$$

-then, the different waves are back-propagated to the source plane with a back-propagating operator G:

$$P_S(k_x,k_y,z=z_S,\omega)=P_A(k_x,k_y,z=z_A,\omega)G(K,d) \qquad (4)$$

This operator enables the separation of propagative and evanescent components in the sound field:

$$G(K,d)=\begin{cases} e^{j\sqrt{k^2-k_x^2-k_y^2}\,d} & \text{prop waves; } k_x^2+k_y^2\le k^2 \\ e^{j\sqrt{k_x^2+k_y^2-k^2}\,d} & \text{evanescent waves; } k_x^2+k_y^2>k^2 \end{cases} \qquad (5)$$

Filtering operations in the wavenumber domain are necessary in order to avoid the extra-amplification of noise with evanescent components. This is performed by means of a Veronesi filter which acts as a low-pass filter in the wave-number domain. Moreover, a Wiener filter is applied to remove uncorrelated noise from the references, which are supposed to represent totally the radiated sound field. For further information on filtering aspects, one should refer to references [3], [7], and [8]. A priori knowledge on the sound pressure field measured is required to optimize the choice of the filter parameters as well as the choice of reference positioning. We paid special attention to the choice of these parameters, which are not detailed here.

-finally, the inverse spatial Fourier transform is used to rebuild the acoustical field on the source plane with a good resolution:

$$p_S(x,y,z,\omega)=SFT^{-1}\{P_S(k_x,k_y,z,\omega)\} \qquad (6)$$

One of the advantages of NAH is that the normal velocity field can also be obtained. This is done by using Euler equation, leading to a back-propagating operator of the form:

$$G_{u_Z}(k,d)=\begin{cases}\dfrac{\sqrt{k^2-k_x^2-k_y^2}}{\rho c k}e^{j\sqrt{k^2-k_x^2-k_y^2}\,d} \\ \quad ,\text{for propagative waves}, \; k_x^2+k_y^2\le k^2 \\ \dfrac{\sqrt{k_x^2+k_y^2-k^2}}{\rho c k}e^{j\sqrt{k_x^2+k_y^2-k^2}\,d} \\ \quad ,\text{for evanescent waves}, \; k_x^2+k_y^2> k^2\end{cases} \tag{7}$$

The same processing as for pressure is used to build the normal velocity field in the source plane u_S:

$$U_S(k_x,k_y,z=z_S,\omega)= P_A(k_x,k_y,z=z_A,\omega)G_{u_Z}(K,d) \tag{8}$$

$$u_S(x,y,z,\omega)=SFT^{-1}\{U_S(k_x,k_y,z,\omega)\} \tag{9}$$

The normal velocity field is obtained on a regular meshing with element length 2.5cm; this computed velocity field is applied as a boundary condition in the radiation model described below.

2.2 The GRIM Method: Classical numerical methods show weaknesses in providing suitable information at all the audible frequencies and thus, in the SIL4 frequency range. Actually, the well-known Finite Element Method well suited to low frequency problems, proves to be unadapted as frequency increases. Besides, Statistical Energy Analysis (SEA) shows difficulties in assessing the vibro-acoustic behaviour of such a complex structure as a helicopter. Geometrical methods have been widely used in the past decades to model the purely acoustic scattering in concert halls. In [9], Jean applied a beam-tracing method to deal with the structural radiation case of a simply supported plate coupled to a room. The results prove to be in good agreement with the results of a boundary element method. This approach was called Green Ray Integral Method (GRIM). In [10], a similar model is developed resting on a partial decoupling hypothesis between the acoustic pressure in a car cavity and the vibration of the car structure in the medium and high frequency range. Based on this hypothesis, the input velocities were measured with an Electronic Speckle Pattern Interferometry (ESPI) measurement system in decoupled conditions. A quite similar approach is proposed here, involving integral formalisms and geometrical concepts. In our case, the velocity field is obtained from the NAH measurement in operating conditions. Moreover, all the supposed radiating panels are measured and the total sound pressure level is calculated as the sum of the sound pressure signals calculated for each panel. The proposed approach is presented below.

Let P(M) be the sound pressure in a closed cavity bounded by surface S_f = (S_V U S_r), where S_V is a vibrating surface of known velocity V and S_r is an acoustic surface with local reaction described by an acoustic impedance Z(ω). The well-known formulation for this problem is:

$$P(M,\omega)=\int_{S_f}\left[G(Q,M,\omega)\frac{\partial P(Q,\omega)}{\partial n}-P(Q,\omega)\frac{\partial G(Q,M,\omega)}{\partial n}\right]dS_f(Q) \tag{10}$$

where G(Q,M,ω) is the free-field Green function between M and any point Q on the surface S_f. A new Green function G_V, solution of the inhomogeneous Helmoltz equation, with the boundary conditions defined in (11) is computed with a beam tracing algorithm, Icare [9].

$$\begin{cases}\left.\dfrac{\partial G_V(Q,M,\omega)}{\partial n}\right|_{S_V}=0 \\ \left.\dfrac{\partial P(Q,\omega)}{\partial n}\right|_{S_V}=\rho j\omega\vec{V}(Q,\omega)\vec{n} \\ \left.\dfrac{\partial G_V(Q,M,\omega)}{\partial n}\right|_{S_r}=\dfrac{jk}{Z(\omega)}G_V(Q,M,\omega) \\ \left.\dfrac{\partial P(Q,\omega)}{\partial n}\right|_{S_r}=\dfrac{jk}{Z(\omega)}P(Q,\omega)\end{cases} \tag{11}$$

With these hypotheses, it is possible to calculate the sound pressure at any position in the cabin due to the vibration of the surface S_V with the following equation:

$$P(M,\omega)=\int_{S_V}j\omega\rho V(Q,\omega)G_V(M,Q,\omega)dS(Q) \tag{12}$$

In this work, all the a priori radiating panels are described as a vibrating surface S_{Vi} with velocity $V_i(Q,\omega)=u_s(x,y,z,\omega)$ measured with NAH (9). The complex pressure $P_{Vi}(M)$ at any point M due to the panel S_{Vi} is calculated with equation (12) and the total sound pressure at point M is generated by:

$$P(M,\omega)=\sum_i P_{V_i}(M,\omega) \tag{13}$$

The summation is made possible because the input velocities used are phased velocity relatively to a fix reference in the cabin.

3. Validation Tests:

In order to validate the presented approach, many tests have to been performed. These tests consist in comparing measurements with simulation results on three separated aspects. In a first part, it is necessary to assess the behavior of Nearfield Acoustical Holography in difficult noisy conditions such as in a helicopter cabin. In a second part, the method coupling NAH and ray-tracing techniques is estimated on a simple test. The latter consist in NAH measurements on 2D isotropic and orthotropic plates in a complex combining an anechoic and a reverberant room. These tests accounted for deriving the best regularization parameters for holographic back-propagation according to our application case. The last test that needs to be achieved is the validation of the acoustical propagation model in the cabin with the beam-tracing technique. This test includes validation of the geometrical modelling of the cabin as well as the definition of absorbing material properties.

3.1 Validation of NAH in noisy conditions:

Actually, acoustic measurements inside a helicopter pose a few difficulties. This section presents the different way to overcome the latter by estimating NAH robustness to difficult measurement conditions.

NAH is originally based upon a measurement of the whole source, in free-field conditions. Nevertheless, for the case of a vehicle interior, this hypothesis can not be checked. In [7], this hypothesis is made true by masking the other faces in order to minimize the acoustic energy coming elsewhere from the face of interest. However, in case of an in-flight-test inside a helicopter cabin, this kind of measurement is not possible for obvious safety conditions. As a consequence, an absorbing and isolating system (Fig.5) was designed to ease the handling of the antenna and to protect the microphones from parasite reflexions on other surfaces. It consists in a rigid plate protected with a foam panel disposed behind the antenna. Another advantage lies in the use of a remote control fixed behind this system. This enables to trigger acquisition easily and hence to increment antenna positions.

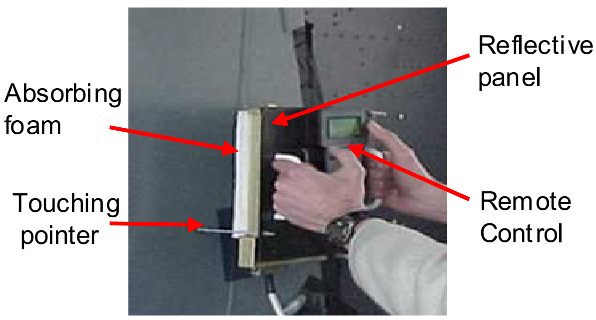

Fig. 5: Absorbing and easy to handle system

The robustness of NAH in noisy conditions such as in a helicopter cabin has then to be checked. This was assessed during a measurement campaign with ONERA in an anechoic chamber on a structure consisting in several loudspeakers excited with a broadband white noise (fig.6).

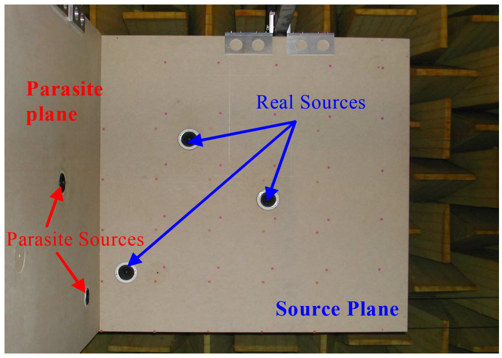

Fig. 6: Test structure

The three loudspeakers in the source plane act as compact sources to detect, and the two sources in the parasite plane generate a perturbation noise. The panels are made of a highly reflective material which tends to increase this background noise. This case simulates the case of an interior vehicle measurement submitted to sound reflexions on side panels. As a reference, a measurement is performed with the 2 parasite sources set inactive (fig.7).

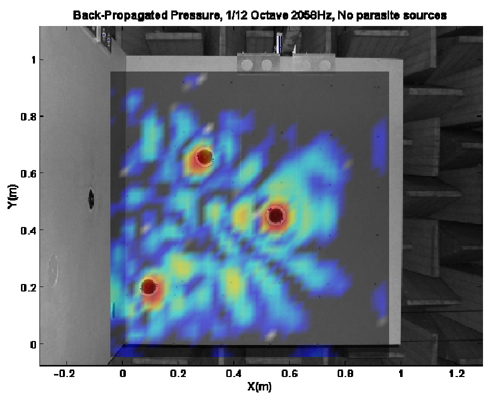

Fig.7: Back-Propagated pressure, 1/12 Octave 2058Hz, without parasite sources

In the case presented below, the 3 loudspeakers in the source plane and the 2 loudspeakers in the parasite plane are excited with a white noise. The results with a SNR of 0dB (that means that the energies generated by the parasite source and the real sources to detect are the same) are presented in the following Fig. 8.

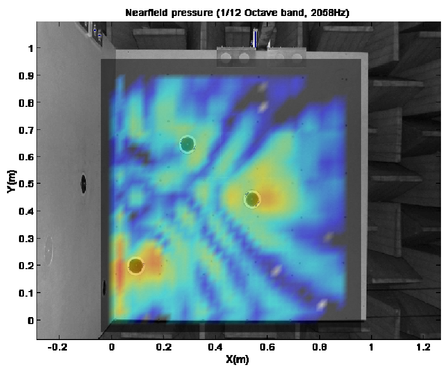

(a)

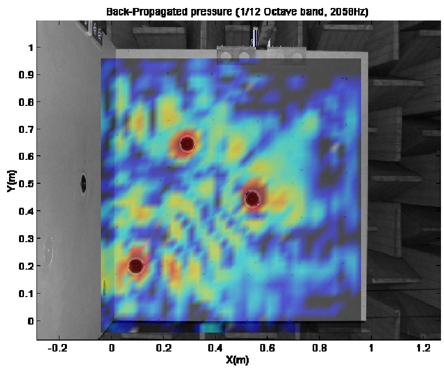

(b)

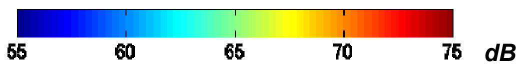

Fig. 8: All Sources correlated (SNR= 0dB). Comparison between Nearfield measurement (a) and back-propagated pressure with NAH (b)

This test provides good information concerning the contribution of NAH to a detailed localization of noise sources in presence of background Noise. The quantitative obtained results are quite good since the max level measured in the source plane without the parasite sources is 74.7 dB (1/12 Octave 2058Hz). It just can be noticed that the used of the absorbing system presented slightly improves the source localization. For further information on the assessment of NAH robustness to difficult measuring conditions, one should refer to [11].

<u>3.2 Validation of the coupling method:</u> The approach presented coupling NAH and the beam-tracing algorithm is first validated on a simple test case in a complex coupling a reverberant room and an anechoic room. This test consists in one vibrating aluminium plate excited by a shaker with a white noise signal. The panel is measured using 25 antenna positions and a reference accelerometer signal is acquired. Recovered velocities in the source plane prove to be in good agreement with the results obtained from a finite element code. A simultaneous acquisition is performed on 2 microphones positioned in the anechoic chamber. In [10], a theoretical value of at list 3 elements per wave-length is presented as being a reasonable value for the numerical integration. With this hypothesis, we can reasonably simulate the plate radiation from the velocity measurements until 4300Hz due to the spatial resolution of NAH results. However, in practice, good results are achieved from 300 to 6400Hz.
The measured and calculated pressures are compared on the microphones in the anechoic chamber. Results are presented on the figure 9 below.

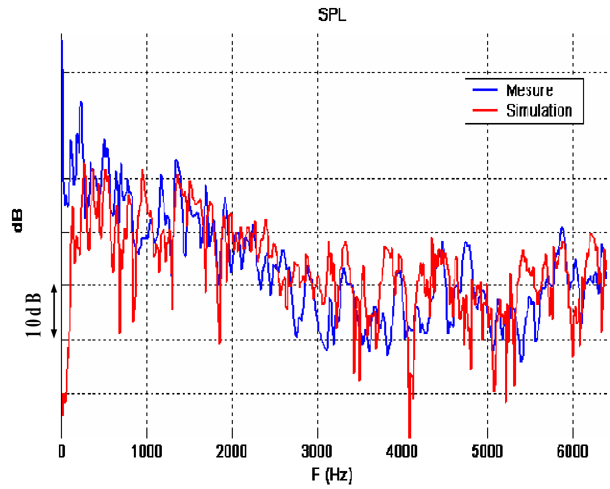

Fig. 9: Comparison measure / simulation on a 2D isotropic plate

The calculated acoustic pressures prove to be in good agreement with the measurement results.

<u>3.3 Validation of the propagation model:</u> In order to assess the validity of the acoustical propagation model in the cabin, some tests using point-like sources have been performed inside a helicopter. The modelling of the test configuration includes the geometrical model of the cabin, the acoustical impedances of the cabin materials, the positioning of sources (loudspeaker) and receivers (microphones at passenger's ears), and a measurement of the directivity of the loudspeaker. The impedances of materials in the cabin have been measured with an impedance tube using a transfer function method ([12]). The test conditions are summarized in the following figure 10.

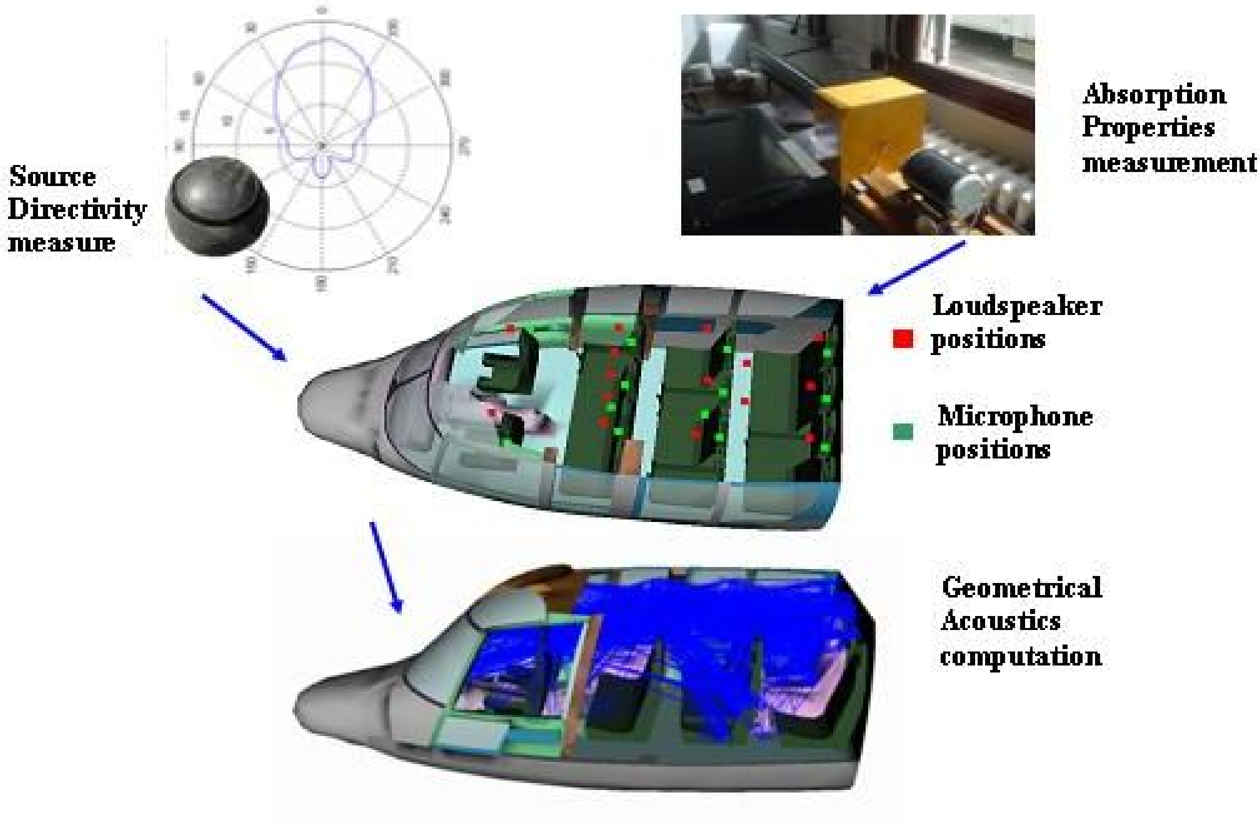

Fig. 10: Validation of the propagation model in the cabin

Figure 11 shows the results of the calculation of the transfer function between a HP input signal and the sound pressure at the passenger's ears locations. This example permits to estimate the ability of geometrical acoustics to compute the Green function in a cavity. It can be shown that a maximum number of 5 wave reflexions by acoustical ray path is enough to meet satisfying results in our case (acoustic convergence of the model).

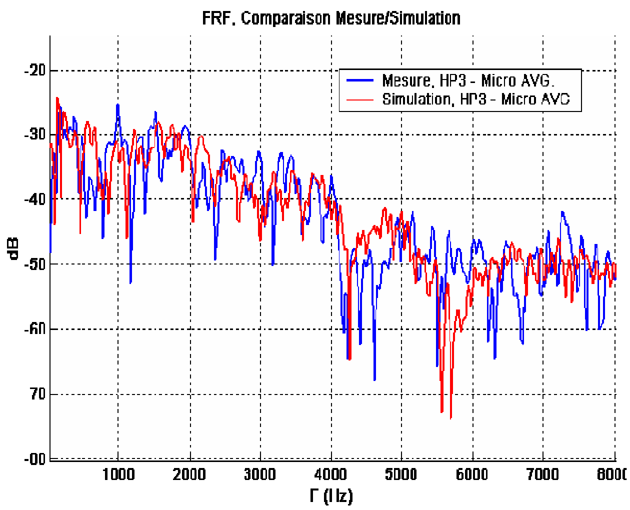

Fig. 11 – Comparison measure / simulation on the FRF computation test

Finally, the obtained results allows for a good confidence in the model consisting in geometry and absorption properties of materials.

4. Measurements on a helicopter:

4.1 Practical implementation: A considerable amount of work lies in the NAH measurement preparation. Practically, measurements are made with a handy square antenna of 8 by 8 microphones spaced out of 2.5 cm. This geometry governs the frequency range available for the measurement results (until 6400Hz). One of the advantages of using a handy array limit transmitted vibrations from the helicopter framework and prevent from the complexity of using a robot inside a helicopter cabin in-flight. The references [13] and [14] discuss the limitations implied by the positioning of antenna. The conclusions drawn are taken into account here.

The measurement series are carried out by using the DATaRec A480 Recording system and the results are stored on a high storage capacity AIT Band, allowing the simultaneous acquisition of the antenna signals combined to 6 multiple reference (maximum total bandwidth : 1280kHz), as illustrated on Fig. 12.

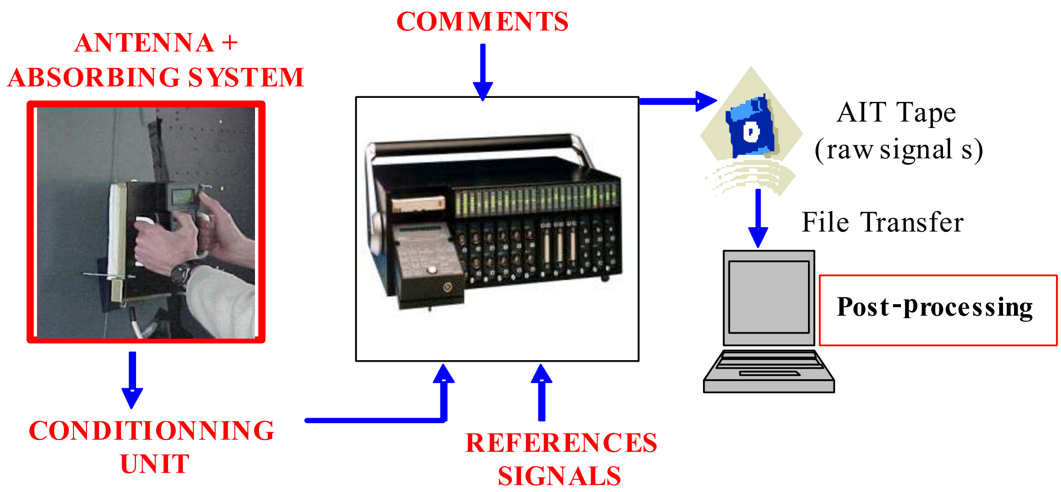

Fig. 12 Microphone Antenna and Acquisition System

The microphone array is positioned successively in front of the cabin panels 7 cm away from the source plane, each position being located thanks to adhesive marks. These positions have been defined in order to avoid problems linked to 2-dimensions measurements on a 3-dimensions geometry, keeping the antenna and the cabin structure as parallel as possible.

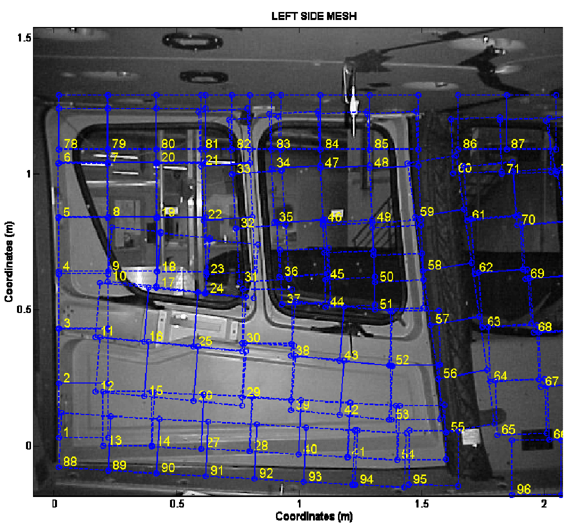

Fig. 13 – Antenna positions mesh

For each new antenna position, an event is triggered on the acquisition system which is easy to locate on the AIT tape. NAH is applied in a post-processing step. For the whole cabin measurement, 405 antenna positions are required (or 25920 microphone positions), for a measurement lasting approximately 1.5 hours.

A particular requirement of the NAH measurement is that signals must be stationary. In order to deal with this difficulty, the spectral matrix used for the NAH post-processing operation is built with at least 50 averages (with 60% overlapping). The compromise between frequency resolution and average number implies that at least 5 seconds should be acquired for each position. However, some thresholds are used to detect remaining non-stationary conditions. In case this threshold is overcome, we have proposed a normalization method: it consists in replacing the pressure input signals with signals normalized by one of the fixed reference signal acquired during the same measurement position.

On a modeling point of view, measuring surfaces are decomposed in several panels for which we want to determine the contribution upon the interior noise level. These panels are positioned so as to fit the real geometry.

<u>4.2 On-Ground measurements:</u> The coupling technique presented in section 2 is tested for ground measurements on a whole helicopter. One of the interests of these tests was to assess the behaviour of the method in realistic reverberant conditions. Another objective was to access to the acoustical radiation of system components, through a measurement series made inside the cabin, with a physical artificial excitation situated on the outside. Different kinds of excitation were checked. We present here the results of a measurement on the rear panel of the cabin submitted to a broadband acoustic excitation in the baggage compartment.

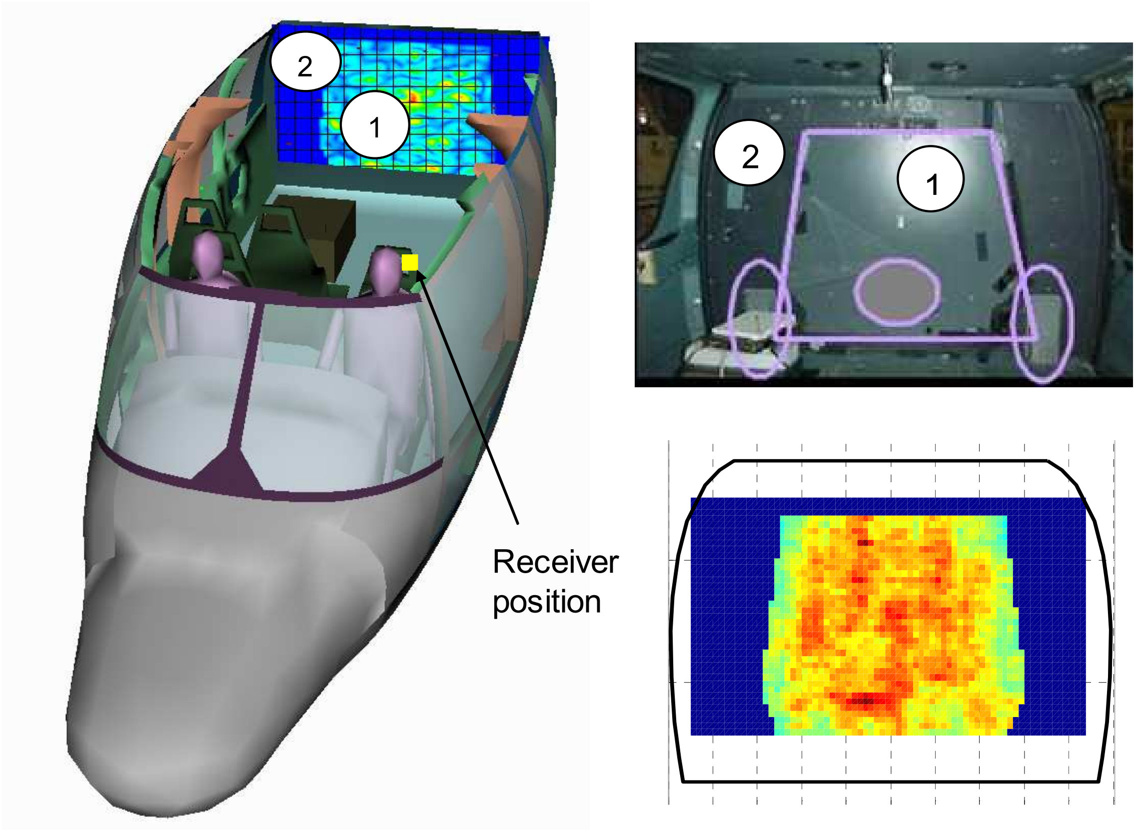

Fig. 14 – Source Decomposition and spatial filtering on the rear panel of the cabin

Three microphones are positioned in the cabin in order to estimate the quality of the coupling method results. The rear panel is divided into 2 plane vibrating surfaces (See Fig 14). Because the surfaces sources introduced in the propagation model have to be rectangular shaped, a spatial filtering operation is necessary in order to define properly each panel contribution. This filtering operation has been implemented in Matlab.

Equation 13 is then used to sum the contribution of the sources 1 and 2. Fig. 15 presents a comparison between the computed and measured signals at copilot position, showing good prediction results. For low frequencies (below 300Hz), the geometrical approach is known for being inaccurate.

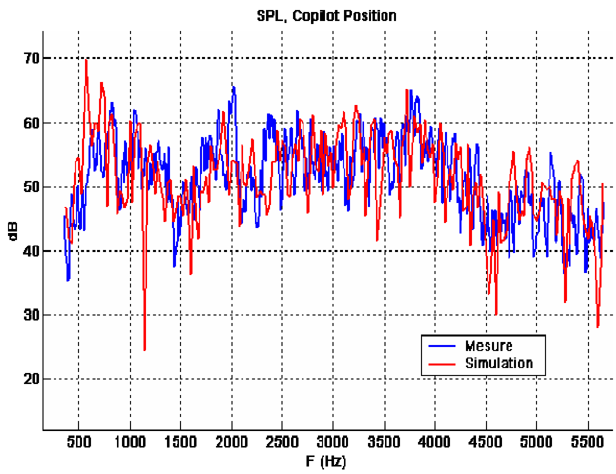

Fig. 15 – Comparison measurement / simulation

Fig. 16 presents the contribution of source 1 and source 2 defined above on the total sound pressure level at copilot position, leading to the conclusion that source 1 is preponderant. The results are in good agreement with the foreseen results.

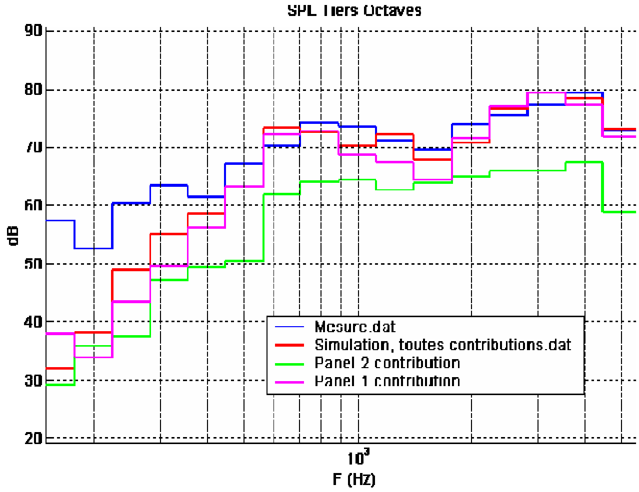

Fig. 16– Contribution of Panel 1 and Panel 2, Third-Octave spectrum.

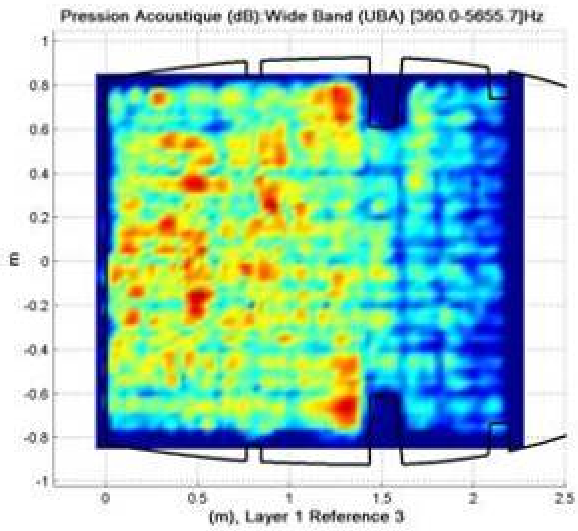

Without trim panel

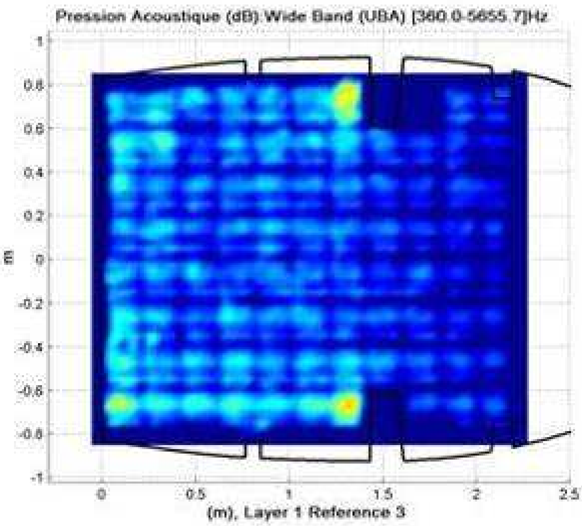

With trim panel

Fig. 17– In-flight results, performance of trim panels

<u>4.3 In-Flight measurements:</u> Finally, the method was applied for a complete diagnosis of helicopter cabin noise. Reference transducers are positioned around the main sources according to the results obtained from a previous microphone measurement campaign. The references which present the best coherence with the cabin microphones are used as fixed references for the holographic treatment. Moreover, extra microphones are positioned inside the cabin at passenger's ears location in order to capture a fully coherent acoustic field. An example of the measurement results obtained is given on the following figure 17, presenting both results on the roof panel without and with trim.

The expected noise sources are well detected, and it allows for a good knowledge of the main radiating zones. The contribution of a total of 21 panels is then simulated in order to rebuild the total sound power level in the cabin. Computed acoustic pressure at passenger's ears locations are compared with microphone measurements. Fig.18 shows the obtained results that validate the effectiveness of the method, comparing the measured and computed results at two different locations in the cabin.

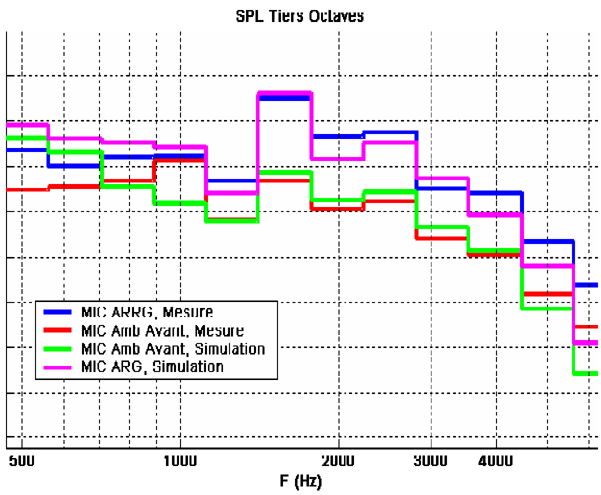

Fig. 18– Total acoustic pressure computed vs measured, Third-Octave spectrum.

Conclusion:

We presented methods developed in order to get a better knowledge of the vibro-acoustic phenomena in helicopters in the medium and high-frequency range. On the one hand, we focused on the contribution of main real acoustic sources on the interior noise levels based on parametric considerations and on conditioned spectral analysis. On the other hand, we presented a radiation model for the helicopter structure coupled to the cabin in the medium and high frequency range, based on the coupling of integral and geometrical concepts. Both measurements and numerical aspects have been discussed and validated on simple test cases and the global methodology has been assessed on the helicopter case. Finally, the in-flight results obtained permit accurate source localization as well as the ranking of the effect of the radiating panels. Therefore, this study improves the knowledge of the vibro-acoustic behavior in the medium and high frequency range. As a perspective, this work should be extended in order to estimate the acoustic incidence of structural modification, and, thus, to improve "acoustical material" type and positioning in the cabin. This global methodology should lead to a better choice of passive treatments to significantly improve the acoustical comfort in helicopter cabins.

REFERENCES:

[1] J-C Pascal, Les techniques d'imagerie acoustique et l'holographie acoustique, Journée imagerie acoustique appliquée, CRITT-M2A, 5 Novembre 2002.

[2] J. Caillet, F. Malburet, J-C.Carmona, F. Marrot: Diagnosis, analyse and modelling of noise paths in a helicopter cabin, *2ème colloque d'analyse vibratoire expérimentale*, Blois, France, 2003.

[3] Maynard, J.D, Williams, E.G. and Y.Lee, Nearfield Acoustical Holography: 1.Theory of generalized Holography and the development of NAH, J.A.S.A 1395-1413,1985.

[4] J. Hald, STSF - a unique technique for scan-based Near-field Acoustic Holography without restrictions on coherence, B&K Technical Review No. 1, pp 1-50, 1989.

[5] J.S Bendat et A.G Piersol, *Engineering applications of correlation and spectral analysis*. New-Yors: Wiley-Interscience, 1980, 302p.

[6] E.G. Williams, B.H. Houston, P.C. Herdic, R. Raveendra, B. Gardner, Interior near-field acoustic holography In flight, J.A.S.A 108, 1451-1463, 2000.

[7] D.Vaucher de la Croix, P.Chevret, F.Perrin, Use of Acoustical Holography in 3D Interior measurements, Proceedings of Inter-noise 2002, Dearborn, MI, USA,19-21 Août 2002.

[8] W.A. Veronesi, J.D Maynard, Nearfield Acoustical holography, II.Holographic reconstruction alogorithms and computer implementation, Journal of Acoustical Society of America **81**(5), 1987.

[9] P. Jean, Coupling integral and geometrical representations for vibro-acoustical problems, J.S.V 224(3), 475-487, 1999.

[10] C Floc'h, A Bardot, X Bohineust, J-D Polach, Vibro-acoustic simulation using geometrical acoustics in the medium frequency range inside a car cavity, Proceedings of Inter-Noise 2000, Nice, FRANCE, 27-30 Août 2000

[11] J.Caillet, F. Marrot, P. Dupont, F. Malburet, J-C.Carmona, Nearfield Acoustical Holography measurement inside a helicopter cabin, European Test & Telemetry Conference, Toulouse, France, 2005.

[12] European Standard, Determination of sound absorption coefficient and impedance in impedance tubes – Part 2: Transfer function method (ISO 10534-2), 1998.

[13] S.M Dumbacher and D.L Brown, Practical Aspects of making NAH measurements, *Society of Automotive Engineers*, 1998.

[14] S.-C. Kang, J.-G. Ih, Y.-J. Park, Near-field limit in positioning the microphone for pressure measurements in using the nearfield acoustical holography *Proceedings of Inter-noise* 2000, Nice, France, 2000.